

Label-free fluorescence aptasensor for chloramphenicol based on hybridization chain reaction amplification and G-quadruplex/*N*-methyl mesoporphyrin IX complexation

Wentao Zheng ^{a,#}, Yubin Li ^{b,#}, Liting Zhao ^b, Ciling Li ^b, Lei Wang ^{a,*□}

^aZhanjiang Central Hospital, Guangdong medical university, Zhanjiang, 524045, China.

^b Faculty of Chemistry & Environmental Science, Guangdong Ocean University, Zhanjiang, 524088, China.

Table S1. Sequences of oligonucleotides

| Name | Sequence (5'→3') |
|------------------|--|
| Apt | 5'- <u>ACT TCA GTG AGT TGT CCC ACG</u> GTC GGC GAG TCG GTG GTA G - 3' |
| Apt-C | 5'- <u>GT GGG ACA ACT CAC TGA AGT</u> -3' |
| Initiator-MB | 5'- <u>ACC TTC TTC TACT TCA GTG AGT TGT CCC ACA GAA</u> <u>GAA GGT GTT TAA GTA</u> -3' |
| Hairpin DNA (H1) | 5'- AGG GCG GGT <u>GGG TGT TTA AGT TGG AGA ATT GTA</u> <u>CTT AAA CAC CTT CTT CTT GGG T</u> -3' |
| Hairpin DNA (H2) | 5'- TGG GTC AAT TCT <u>CCA ACT TAA ACT</u> AGA AGA AGG <u>TGT TTA AGT TGG</u> GTA GGG CGG G -3' |

Spectra properties of samples were detected under the same experimental conditions using an F-4600 Hitachi fluorescence Spectrometer with a xenon lamp. At an excitation of $\lambda = 399\text{nm}$, the emission peak was recorded at 612 nm both for *N*-Methyl mesoporphyrin IX(NMM) and NMM/G4 (Figure S1). However, the fluorescence intensity of NMM/G4 was significantly higher than that of NMM, indicating that the NMM/G4 composite greatly enhanced the fluorescence of NMM.

* Corresponding author. E-mail addresses: wangleigdmu@163.com (Lei Wang)

Wentao Zheng and Yubin Li contributed equally to this work.

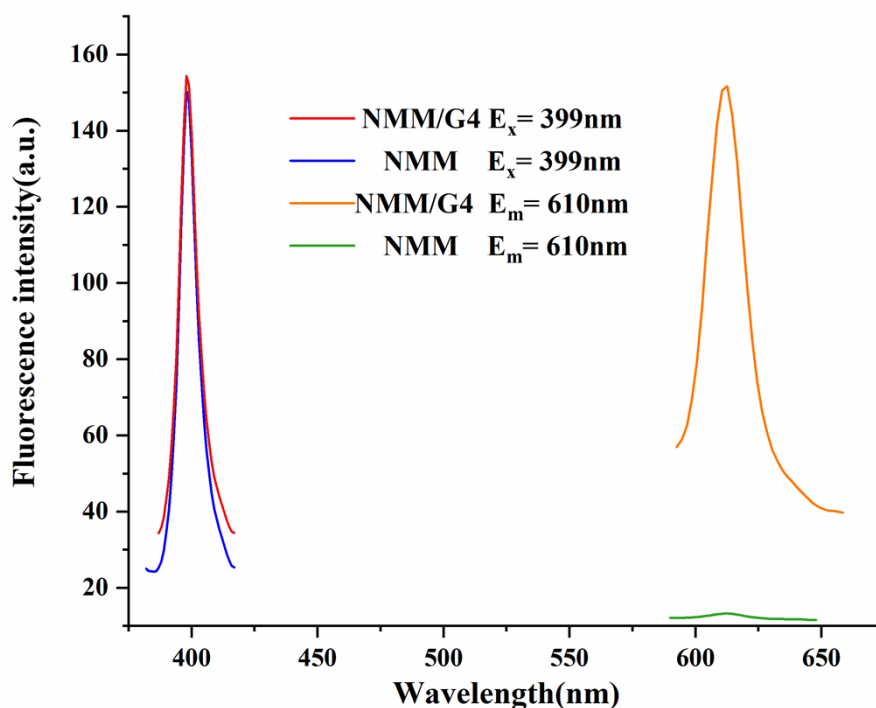


Figure S1. Spectra properties of NMM and NMM/G4

The fluorescence intensity of NMM was enhanced after the complexation reaction with G-quadruplexes. The systematic quantum yield was measured for G4/ NMM, and the quinine sulfate dihydrate which dissolved in 0.1 mol/L H₂SO₄ with a quantum yield of 51% was the reference. The quantum yield (y) is calculated by the following formula.

$$Y = Y_R \cdot \frac{F_S \cdot A_R \cdot \eta_S^2}{F_R \cdot A_S \cdot \eta_R^2}$$

F is the integral area of the fluorescence emission spectrum, A is the absorbance, and η is the refractive index of the solvent (R and S represent the reference quinine sulfate dihydrate solution and the sample respectively)

The systematic quantum yield measurements were shown in table S2.

Table S2. Systematic quantum yield measurements

| | Test sample | λ_{ex}/nm | A | F | Y |
|-----------|---------------------------|-------------------|-------|-------|------|
| Reference | quinine sulfate dihydrate | 399 | 0.024 | 13245 | 0.51 |
| Sample | G/NMM | 399 | 0.02 | 15319 | 0.64 |

Table S3. Comparison with other methods for CAP detection

| Method | Detection limit | Detection range | Ref. |
|---|---------------------------|---|--------------------|
| Electrochemiluminescence assay | 1.7 pg·mL ⁻¹ | 0.01 - 4000 ng·mL ⁻¹ | (Chen et al. 2020) |
| Structure switching signaling Assay | 0.70 ng mL ⁻¹ | 1 - 100 ng·mL ⁻¹ | (Ma et al. 2020) |
| MOF-based ratiometric fluorescent biosensor | 0.08 pg mL ⁻¹ | 0.1pg ·mL ⁻¹ - 10ng·mL ⁻¹ | (Liu et al. 2020) |
| Electrochemical sensor | 0.32 μmol·L ⁻¹ | 0.03 - 0.5 mmol·L ⁻¹ | (Shad et al. 2019) |
| Photovoltammetric sensor | 0.14 μmol·L ⁻¹ | 0.5 - 50 μmol·L ⁻¹ | (Zhu et al. 2019) |
| Chemiluminescence resonance energy transfer assay | 2.0 pg·mL ⁻¹ | 0.01 - 100 ng·mL ⁻¹ | (Jia et al. 2019) |
| Label free aptasensor based on HCR and G-quadruplex/NMM | 0.8 pg·mL ⁻¹ | 2.5 - 200 pg·mL ⁻¹ | This work |

Chen, J., Zheng, J., Zhao, K., Deng, A., & Li, J. (2020). Electrochemiluminescence resonance energy transfer system between non-toxic SnS₂ quantum dots and ultrathin Ag@Au nanosheets for chloramphenicol detection. *Chemical Engineering Journal*, 123670.

Ma, X. Y., Li, H. X., Qiao, S. N., Huang, C. J., Liu, Q. I., & Shen, Xu. (2020). A simple and rapid sensing strategy based on structure-switching signaling aptamers for the sensitive detection of chloramphenicol. *Food Chemistry*, 302, 125359.

Liu, S., Bai, J. L., Huo, Y. P., Ning, B. A., Peng, Y., Li, S., Gao, Z. X. (2020). A zirconium-porphyrin mof-based ratiometric fluorescent biosensor for rapid and ultrasensitive detection of chloramphenicol. *Biosensors and Bioelectronics*, 149, 111801.

Shad, N. A., Bajwa, S. Z., Amin, N., Taj, A., Hameed, S., Khan, Y., Dai, Z., Khan, W.S. (2019). Solution growth of 1D zinc tungstate (ZnWO₄) nanowires; design, morphology, and electrochemical sensor fabrication for selective detection of chloramphenicol. *Journal of Hazardous Materials*, 367, 205-214.

Zhu, Y. H., Yan, K., Xu, Z. W., Wu, J. N., & Zhang, J. D. (2019). Cathodic “signal-on” photoelectrochemical aptasensor for chloramphenicol detection using hierarchical porous flower-like Bi-BiOI@C composite. *Biosensors and Bioelectronics*, 131, 79–87.

Jia, B. J., He, X., Cui, P. L., Liu, J. X., & Wang, J. P. (2019). Detection of chloramphenicol in meat with a chemiluminescence resonance energy transfer platform based on molecularly imprinted graphene. *Analytica Chimica Acta*, 1063, 136-143.